Research article

Wnt/β-catenin signaling pathway is activated in the progress of mandibular condylar cartilage degeneration and subchondral bone loss induced by overloaded functional orthopedic force (OFOF)

Zijing He [a,b,1], Meixi Liu [c,1], Qiang Zhang [a,b], Yihong Tian [a,d], Lingzhi Wang [a,b], Xiao Yan [a,b], Dapeng Ren [a,b], Xiao Yuan [a,b,*]

[a] Department of Orthodontics II, The Affiliated Hospital of Qingdao University, Qingdao, China
[b] School of Stomatology of Qingdao University, Qingdao, China
[c] The Center of Stomatology, Qingdao Municipal Hospital Affiliated to Qingdao University, Qingdao, Shandong, China
[d] State Key Laboratory of Oral Diseases and National Clinical Research Center for Oral Diseases Department of Orthodontics West China Hospital of Stomatology, Sichuan University, Chengdu, China

A R T I C L E   I N F O

A B S T R A C T

Objective: To explore the role of Wnt/β-catenin signaling pathway in the pathogenesis and progression of temporomandibular joint osteoarthritis (TMJ OA) caused by overloaded force.
Materials and methods: We generated a rat model of forward mandibular extension device to induce TMJ OA by overloaded force. Condylar cartilage samples were collected at 2wk, 4wk, and 8wk after appliances were installed. Changes of the condylar cartilage and subchondral bone were evaluated by hematoxylin and eosin (HE), Safranin O and Fast Green staining (SO&FG), micro-CT, tartrate resistant acid phosphatase (TRAP) staining. The expression levels of β-catenin, COL-2, MMP3 and sclerostin (SOST) were detected by immunohistochemistry (IHC) and PCR.
Results: HE, SO&FG, micro-CT, OARSI and Mankin scores showed that the condyle cartilage layer was significantly thinner and proteoglycan loss in the overloded group. TRAP staining exhibited that the number of positive osteoclasts increased and OPG level decreased in the overload group. IHC, PCR showed that the expression of COL2 and SOST decreased, while MMP3 and β-catenin increased in the overload group.
Conclusion: Wnt/β-catenin signaling pathway is activated in the progress of mandibular condylar cartilage degeneration and subchondral bone loss induced by overloaded functional orthopedic force (OFOF)

1. Introduction

Among all malocclusions, class II malocclusion is a persistent challenge for orthodontists [1]. The functional appliance has become the first choice for pre-adolescent children or adolescents with Class II malocclusion due to it's remodeling function at the glenoid fossa and mandibular condyle, resulting in a repositioning of the condyle as well as may cause mandibular autorotation [2]. Previous studies indicated that long-time functional orthopedic treatment could induce pathological changes of the condyle, and lead to temporomandibular joint diseases (TMDs) [3, 4, 5]. TMD can progress to temporomandibular joint osteoarthritis (TMJ-OA), it will lead to severe dysfunction and pain. The

progressive degeneration of mandibular condylar cartilage (MCC) is commonly associated with synovial inflammation and subchondral bone loss, which is the main characteristic of TMJ disease [6]. Animal models have proofed different processes and degrees of mandibular condylar cartilage degeneration through different overloading forces on TMJ of animal models to build steady mouth opening [7], occlusal disorder [8], or resistant food [9]. Besides, the steady mouth-opening model has been applied in rats, mice, and rabbits with good operability and repeatability [8, 9, 10, 11]. Early adaptive proliferation of cells in mandibular condylar cartilage was found with this model, and the degeneration of cartilage progressed with the extension of induction time [10, 11, 12]. But it is not a suitable model to mimic the overloaded functional orthopedic force

---

(OFOF) to guide the mandible advancement. Thus, a new animal model should be generated to explore the process of mandibular condylar cartilage after guiding the mandible advancement.

The Wnt/β-catenin signaling pathway is a crucial role in regulating cartilage metabolism and disease, and it regulates chondrocyte proliferation and function under physiological conditions [13]. In addition, abnormal active of the Wnt/β-catenin pathway can induce chondrocyte hypertrophy and lead to degeneration of the articular cartilage by expressing the catabolic factors such as VEGF, MMP-13, COLX, and ADAMTS-5 [14, 15]. Activation of Wnt/β-catenin signaling pathway promotes hypertrophic differentiation of chondrocytes, thereby inducing cartilage degradation and exacerbating OA progression [16]. Sclerostin has been shown to be an endogenous Wnt/β-catenin inhibitor that maintains cartilage integrity in a mouse model of OA [10, 17]. Another study also suggested that sclerostin plays a protective role by inhibiting Wnt [6].

In previous studies, there were many studies on the regulation of cartilage metabolism by WNT signaling pathway, but there were few studies on the temporomandibular joint. In this study, we generated a rat model with the mandible in the protruded position to mimic the TMJ OA caused by overload functional orthopedic force (OFOF). Using this model, we observed the changes in the condylar cartilage and subchondral bone of the TMJ, explored the role of the Wnt/β-catenin signaling pathway in TMJ OA induced by overloaded functional orthopedic force.

2. Materials and methods

2.1. Animals and experimental protocol

All experiments were carried out under the guidelines of the Animal Experiment Committee of Qingdao University. 40 five-week old male SD rats (SPF grade), weighing 160 ± 20 g, were raised by the Animal Experiment. The breeding environment temperature is 20–22 °C, and the environmental humidity is 40–60%. The light day/night cycle is 12 h/d per day. All rats were randomly assigned to four groups (n = 10/group): control, 2wk (MA for 2 weeks), 4wk (MA for 4 weeks), and 8wk (MA for 8 weeks). During the adaptation period, the rats received food and water ad libitum, but during the experiment, to prevent the appliance from being removed, the rats only ate during the dark period. MA (Figure 1A) was performed by an appliance designed by Yang J et al. [13] In brief, the device consists of three parts: an upper-incision crown, an inclined guide plate, and an extraoral auxiliary retention device. Every time the rat closed its mouth, the mandible moved forward along the inclined plane, which was consistent with the principle of functional orthopedics. The rats wore a baffle with a border to prevent appliances from being removed (Figure 1B). Schematic diagram of rat mandibular advanced has been shown in Figure 1C.

2.2. Tissue preparation

The rats were sacrificed on Ctrl, 2wk, 4wk, and 8wk with the appliance (Table 1). The rats were killed by carbon dioxide gas (Aligal 2, Air Liquid, Sydney, Australia). The left condyle was anatomically separated from the surrounding structures immediately after death, and the excess tissue around the condyle was removed. Rinse with PBS for twice, fix in paraformaldehyde for 24 h, decalcify with 10% EDTA for 30 days, and embed the specimen after dehydration. 5um serial sections were prepared along the mid-sagittal plane of the condyle for histological and immunohistochemical staining. The right condyle was fixed in 4% paraformaldehyde, then was analyzed by micro-CT. For each group, the condylar of the 6 TMJ from 3 rats were separated for RNA extraction and store the sample at -80 °C. The condyle subchondral bone 3mm below the cartilage-bone junction was transected and RNA extraction was collected.

2.3. Histological staining and scoring

Hematoxylin and eosin staining (HE) and Safranin O and Fast Green staining (SO&FG)staining were used to assess the condylar histological

changes. The surface of the condylar cartilage is evenly distributed between the anterior, middle, and posterior third of the distal joint of the condyle and between the anterior and posterior joints. Three squares (300 μm × 300 μm) of central two-thirds of the condylar cartilage covering all hypertrophic layers was applied. Cartilage thickness was measured in the central third. Condylar cartilage were scored by the OARSI and Mankin scoring system [15, 16].

2.4. Immunohistochemistry and TRAP assay

Expression of COL-2, MMP3, SOST, β-catenin on condylar was measured and described by immunohistochemical analysis. Sections were dewaxed, washed and rehydrated with standard xylene ethanol, and sealed with phosphate buffered saline (PBS) and FBS. After blocking, sections were incubated with SOST specific primary antibody overnight (1:100 dilution, Abcam), β-catenin (1:100 dilution, Cell Signaling Technology), MMP-3 (1:100 dilution, Abcam) and COL2A1 (1:100 dilution, Abcam). Prepared negative control with PBS instead of primary antibody. Incubated with secondary enzyme-conjugated anti-rabbit IgG (cell signaling technology, Boston, USA), and stained with 3,3′-diaminobenzidine tetramine hydrochloride and hematoxylin reverse staining. The stained sections were analyzed under a Leica DM 2500 microscope. TRAP staining was performed on each slide in each group to assess osteoclast activity (Sigma, USA) [6]. TRAP staining was used to explore the osteoclast activity of the subchondral bone of the condyle. Five field TRAP + osteoclasts under high power (400 ×) microscope were randomly selected, and the average value was taken.

2.5. Micro-CT

Scan the rat condyle heads by a micro-CT system (Latheta LCT 200, Hitachi, Japan). In the position of the middle and posterior part of the subchondral bone of the condyle, select two cubes with a size of 0.25 × 0.25 × 0.25 mm, and use Mimics software to reconstruct them, and calculate the relevant bone parameters of these two areas such as: bone volume to total volume (BV/TV), trabecular bone thickness (Tb. Th), trabecular bone number (Tb. N), trabecular bone space (Tb. Sp), and then the data for trabecular microstructural between different experimental groups was analysis.

2.6. Detection of mRNA levels

Total RNA was extracted using Trizol (Thermo, MA, USA). Detected gene expression by the real-time PCR machine (7500; Thermo, USA). Calculated the expression level of target gene relative to lyceraldehyde-3-phosphate dehydrogenase (GAPDH). The calculated result (n = 3) is the relative quantification of the target gene relative to the control group, set as 1 [18]. Table2 listed the primers for the target genes.

2.7. Statistical analysis

The experimental data are presented as the mean ± standard deviation (SD) of at least three independent experiments. Results were evaluated by one-way analysis of variance. Statistical significance was defined as* represents $P < 0.05$, ** represents $P < 0.01$, *** represents $P < 0.001$.

3. Results

3.1. Overloaded functional orthopedic force induced the condylar cartilage degeneration process

To examine the condylar cartilage degeneration process after applied overloaded functional orthopedic force in rats for different durations. The condylar cartilage were divided into four layers: ① Fibrous layer: composed of several layers of fibrous cells, with complete surface and less
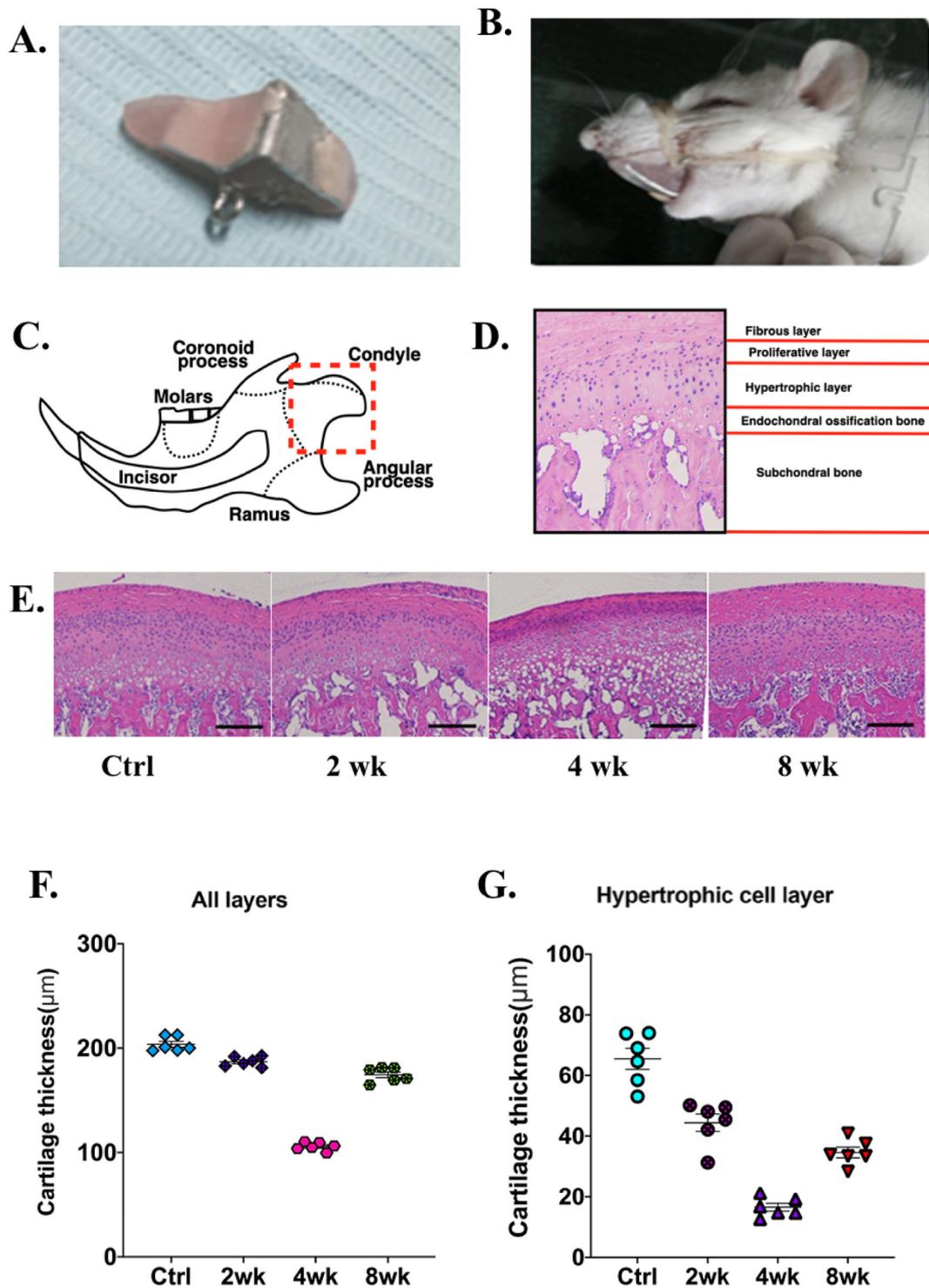
Figure 1. Thickness of the condyle cartilage in the control and overloading groups at 2w, 4w, and 8w. **A, B**: Intraoral views of the mandible advanced appliance model. **C**: Schematic diagram. **D**: Schematic diagram of the histological layer of the condyle head (Fibro fibrous layer; Prolif proliferative layer; Hypertrophic layer, Endochondral ossification bone layer, Subchondral bone layer). The sagittal section of the central condyle was stained with hematoxylin and eosin (× 200). E: All layers of condylar cartilage in the overload group were thinner than those in the control group, especially the hypertrophic layer. **F, G**: Comparison of the total cartilage thickness and thickened layer thickness among all groups. The layers of condylar cartilage, especially the thickened layer, were thinner in the loading group than in the control group. (*P < 0.05, **P < 0.01, ***P < 0.001*).

cell components; ② Proliferative layer: located below the fibrous layer, the cells were small, round or oval, and arranged closely; ③ Hypertrophic layer: composed of mature chondrocytes and extracellular matrix. The cell volume is larger than the proliferative layer, and it is oval. The volume of cells located in the deep part of the hypertrophic layer is further increased, and the extracellular matrix is uniform; ④ The artilage

calcification layer: this layer is the junction of cartilage and subchondral bone, where ossified chondrocytes can be seen (Figure 1D). H&E staining showed that the condylar cartilage surface was intact and smooth in the control group. However, in the group of overloaded, all the condylar cartilage layers became significantly thinner, especially the hypertrophic layer, and it was especially evident in the 4wk group (Fig. 1E, F, G). In the

Table 1. Allocation of rats into the four groups.

Study Criteria	Weeks into Experiment Before Sacrifice	Number of Experimental Rats
Mandible Advancement	Control group	10
	2wk group	10
	4wk group	10
	8wk group	10

4wk group, we observed the vacuolation and degeneration. While in the 8wk group, the cartilage of the condyle showed a gradually increase in the thickness of each histological layer, compared to the 4wk group when the overloading time was prolonged. But each layer of cartilage after 8 weeks of overloading remained reduced compared to the control group (Fig. 1E, F, G).

SO&FG staining showed the same trend. Red staining showed more obvious changes in the number of chondrocytes and matrix expression in deep layer. In addition, Safranin-O staining was used to visualized the situation of proteoglycan loss (Figure 2A). At 2wk, 4wk and 8wk, OA scores were significantly elevated (OARSI and Mankin scores), suggesting that the temporomandibular joint showed a degenerative phenotype at different time points, accompanied by overload (Figure 2B). The score of the 4wk group was higher than that of the other groups. The trend of OARSI score was consistent to the Mankin score.

3.2. Overloaded functional orthopedic force aggravated the loss of the extracellular matrix in condylar

COL-2 was mainly distributed in prehypertrophic and hypertrophic layers (Figure 3A). The express of COL-2 was significantly reduced by overloaded orthopedic force in condylar cartilage. While we found that the significant decreased was in the 4wk group compared with the control group, 2wk and 8wk group (Figure 3B, $P < 0.001$ and $P < 0.01$ respectively). Moreover, compared with the control group, COL-2 expression decreased significantly in the 8wk group (Figure 3B, $P < 0.01$). But after 4 weeks of overloading, COL-2 expression became significantly increase. 8wk group was significantly increasing more than 4wk group (Figure 3B, $P < 0.01$).

The expression of MMP-3 in the loading group was significantly increasing than that in the control group, further the change was the most significantly in the 4wk group (Figure. 3A,C). Moreover, compared with the 4wk group, the MMP-3 expression was decreased in the 8wk groups ($P < 0:01$) (Figure 3C).

3.3. Effects of overloaded functional orthopedic force on subchondral condylar bone

Micro-CT images (sagittal plane, horizontal plane) showed that the subchondral bone of the condyle had obvious bone resorption in the overloaded group compared with the control group. The size of the condyle head of the overloaded group was significantly smaller than that of the control group, especially the width of the condyle head. Images of micro-CT showed progressive destruction and severe subchondral bone loss with prolonged induction (Figure 4A). The subchondral bone showed significant differences in BV/TV, Tb.Th, Tb.N, and Tb.Sp

(Figure 4B). A significant decrease in BV/TV, Tb.Th and Tb.N was observed in the 4wk group. Compared with 4wk group, while increased in the 8wk group. Tb.Sp increased gradually, the highest Tb.Sp values were observed in the 4wk group.

3.4. Effects of overloaded functional orthopedic force on osteoclast activity in condyle subchondral bone

To figure out the role of osteoclasts in the onset phase of TMJ OA, in vivo condition, we use TRAP staining to explore the influence of overloaded force to osteoclastogenic activity (Figure 5A). The activity of osteoclasts was quantified by the number of TRAP-positive osteoclasts in the condylar subchondral bone. TRAP-positive cells were mainly distributed on the inferior surface of cartilage and near bone marrow were observed mainly in bone marrow, adjacent to the subchondral surface (Figure 5A). For the samples analyzed from overloaded group, the number of TRAP-positive osteoclasts increased, while the significant increase was the most in the 4wk group (Figure 5B, $P < 0.001$ and $P < 0.01$ respectively), thereby indicating that osteoclast activity was significantly aggravated after overloaded force. But after 4 weeks of overloading, the number of TRAP-positive osteoclasts began to significantly decrease. The decreasing level of 8wk group was more obvious than 4wk group, but it was still in a significantly high level compared with the control group (Figure 5B). Consistent with TRAP staining results, Real-time PCR analysis further showed that the expression of osteoclast marker RANKL was elevated. The RANKL mRNA levels of 2wk, 4wk and 8wk group were significantly increased compared to the control group, the significant increase was found in the 4wk group. Meanwhile, the levels of OPG were reduced. In the overloading groups, mRNA levels of RANKL expression were significantly increased, while OPG in cartilage or subchondral bone were reduced, resulting the RANKL/OPG ratio increased in cartilage and subchondral bone compared with the control group (Figure 5C). Taken together, these results suggested that overloaded functional orthopedic force is able to effectively increase osteoclast activity.

3.5. Overloaded functional orthopedic force activated Wnt/β-catenin signaling pathway by upregulating the expression of β-catenin in aggravating cartilage degeneration

We examined the expression of sclerostin and β-catenin in cartilage by immunohistochemistry to investigate whether overloaded functional orthopedic force intensifies cartilage degeneration by activating β-catenin (Figure 6). The results showed that positive staining of sclerostin decreased at 2wk, 4wk and 8wk group, while the significant increase of β-catenin was found in the 4wk group compared with the control group, 2wk and 8wk group (Fig. 6A,C). Moreover, the expression patterns of sclerostin and β-catenin were negatively correlated, the positive staining of β-catenin was significantly increased after overloading, the significant increase was found in the 4wk group when compared with control group, the 2wk and 8wk group (Fig. 6B,C).

To determine the expression level of sclerostin and β-catenin during the progression of TMJ OA induced by overloaded force, we compared their expression level with qRT-PCR analysis. The expression of sclerostin (SOST) was significantly decreased at 2wk, 4wk and 8wk group, as compared with the control group (Figure 6D). In addition, the levels of β-catenin mRNA in TMJ OA cartilage were higher in overloaded group

Table 2. Sequences of primers of target genes used for real-time PCR.

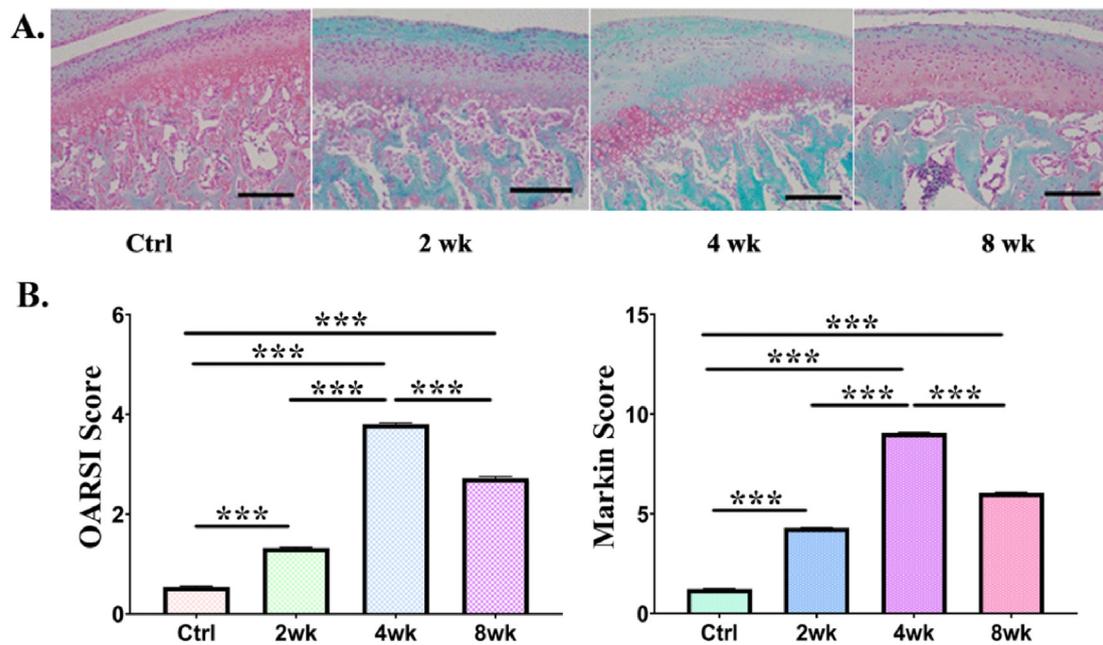| Target gene	Forward primer	Reverse primer
RANKL	5′-GGCTTACCTGCCCAGTCTCATC-3′	5′-AAGCATCATTGACCCAATTCCAC-3′
OPG	5′-TTACCTGGAGATCGAATTCTGCTTG-3′	5′-GTGCTTTCGATGAAGTCTCACCTG-3′
β-catanin	5′-TCACGCAAGAGCAAGTAG-3′	5′-CTGGACATTAGTGGGATGAG-3′
SOST	5′-TGATGCCACAGAAATCATCC-3′	5′-ACGTCTTTGGTGTGCATAAGG-3′
Gapdh	5′-TTCAACGGCACAGTCAAGG-3′	5′-CTCAGCACCAGCATCACC-3′

Figure 2. Degenerative changes was exhibited in temporomandibular condylar in the control and overloading groups in the 2wk、4wk、8wk group. **A:** Safranin-O and fast green staining (× 200). Gradual but significant loss of proteoglycan is observed in the 2wk、4wk、8wk group. In addition, chondrocytes were irregularly arranged and fibrillation were observed at different time points of rat condyles. **B:** Comparison of the OA score (including OARSI and Mankin score) between the groups. The OARSI and Mankin score are significantly higher in the overloading groups than in control groups from 2wk onwards (*P < 0.05; **P < 0.01; ***P < 0.001).
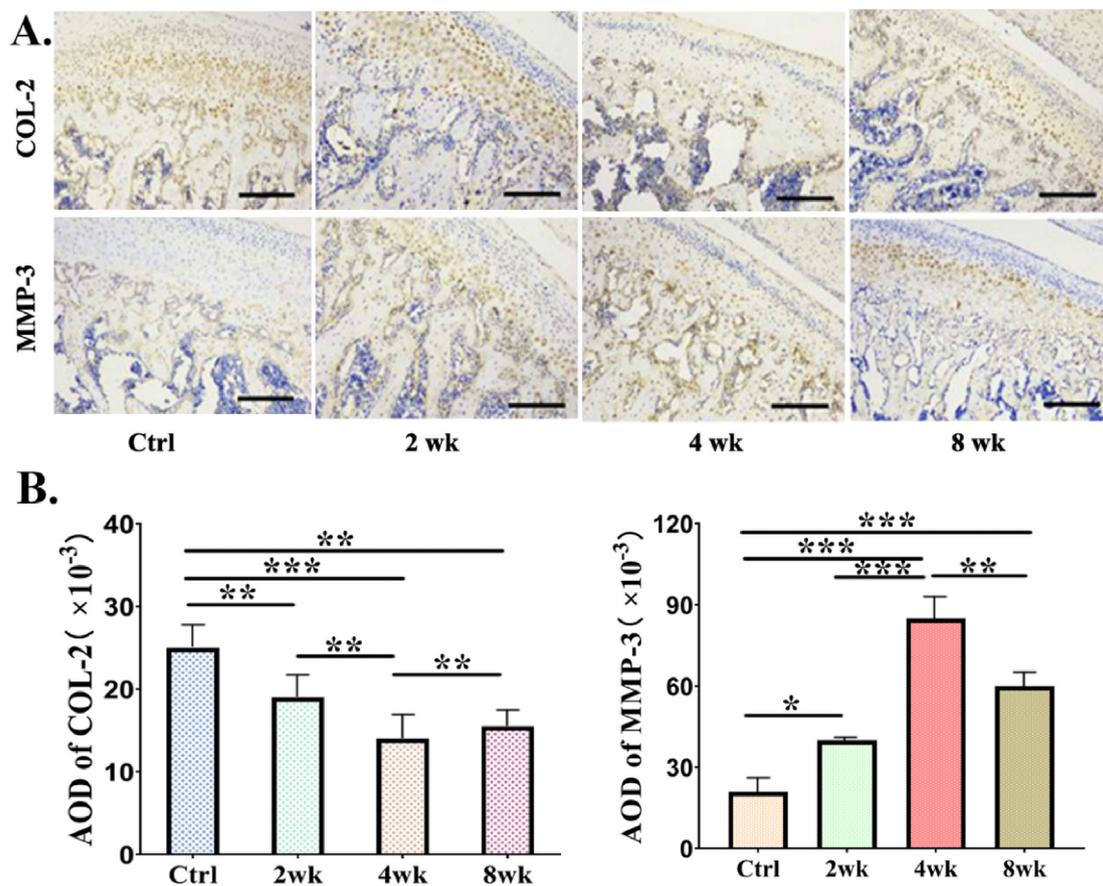

Figure 3. COL-2 and MMP-3 Immunohistochemical staining and percentage comparison of condyle cartilage of COL-2 and MMP-3 positive chondrocytes between different groups. **A:** Immunohistochemical staining and the COL-2 and MMP-3 analysis of quantitative in the condylar cartilage. **B:** Corresponding to the microscopic images, COL-2 expression was significantly decreased in the overloaded groups. The decrease was most significant in the 4wk group. Moreover, compare to the 4wk group, the COL-2 expression was increased in the 8wk groups. **C:** The MMP-3 expression increased to various degrees in the overloaded groups, The change in the 4wk group was most significant. Again, compare to the 4wk group, MMP-3 expression was decreased in the 8wk groups. The data are recorded as the mean ± SD. (*P < 0:05; **P < 0:01. **P < 0:001.
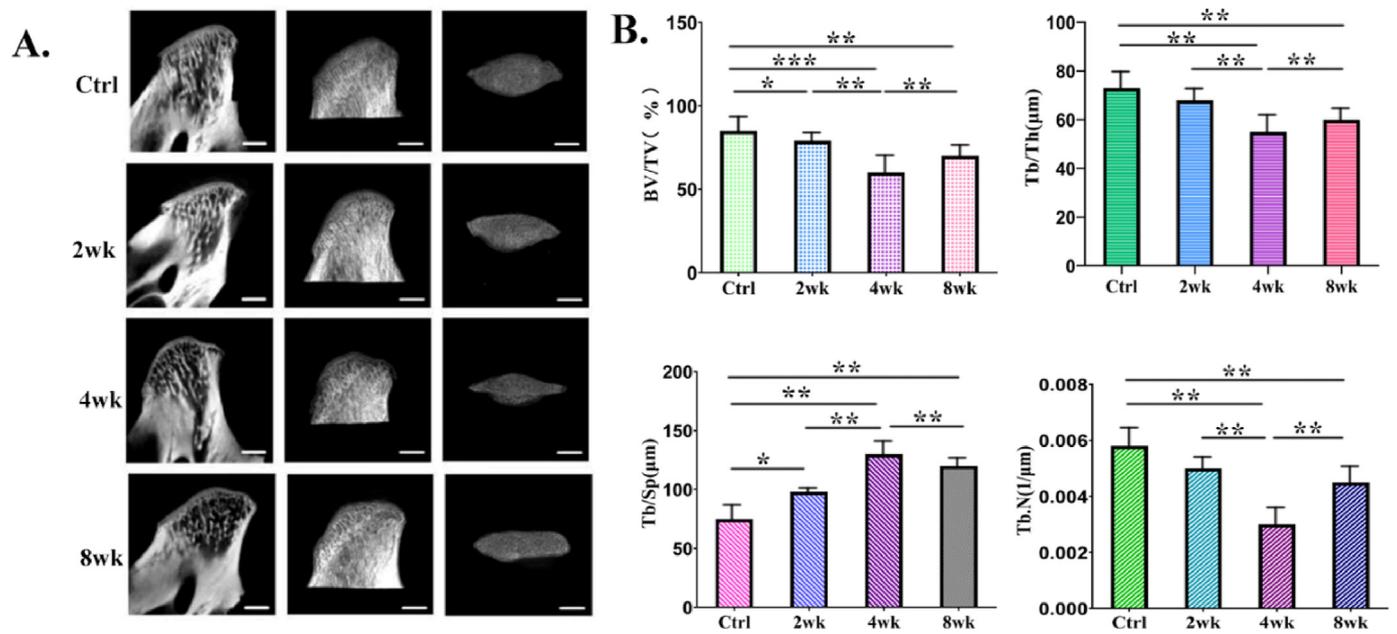
Figure 4. In vivo micro–computed tomography (CT) images and analysis of the subchondral bone resorption at the mandibular condyle induced by overloaded functional orthopedic force. **A**: Sagittal micro-CT image of condyle. **B**: micro-CT measurements for the indicated parameters in the subchondral bone. Bone volume fraction (BV/TV), trabecular thickness (Tb.Th), trabecular separation (Tb.Sp), and trabecular number (Tb.N) were calculated from subchondral cubes. The data were expressed as mean $\pm$ SD and *$P < 0.05$, **$P < 0.01$, and ***$P < 0.001$.
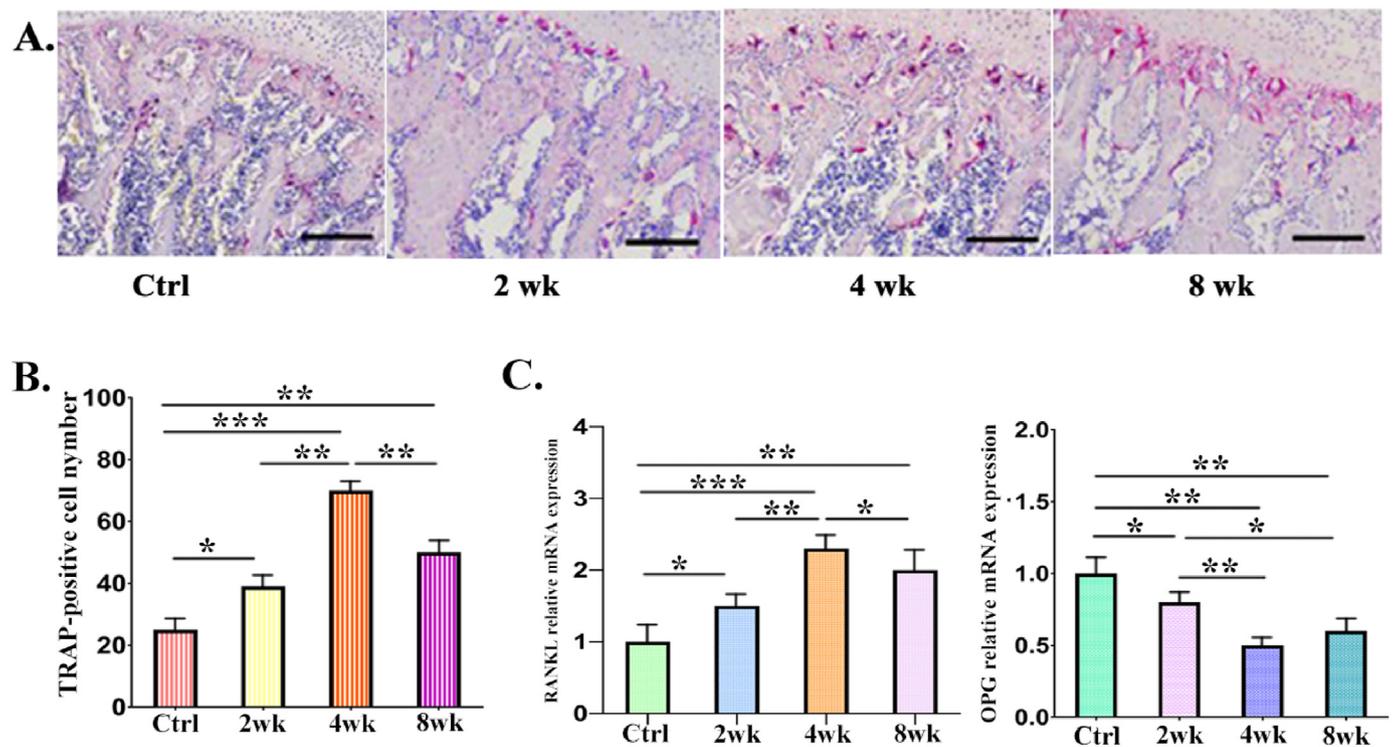

Figure 5. The number of subchondral osteoclasts in mandibular condyle in control group and experimental group. **A**: TRAP staining in the mandibular condylar subchondral bone was performed and multinucleated osteoclasts are indicated. **B**: TRAP-positive osteoclasts of the analysis of quantitative. **C**: Increased mRNA expressing levels of RANK and decreased mRNA expressing of OPG in condylar subchondral bone. The data were expressed as mean $\pm$ SD and *$P < 0.05$, **$P < 0.01$, and ***$P < 0.001$.

than in normal cartilage (Figure 6 D). Changes in sclerostin and β-catenin levels may be related to degeneration of chondrocytes. Wnt/β-catenin signaling pathway is activated in the progress of mandibular condylar cartilage degeneration and subchondral bone loss induced by overloaded functional orthopedic force (OFOF).

4. Discussion

Many mandible advancement (MA) appliances have been used in patients for treatment of mandibular retrognathia. The mechanism of orthodontic treatment of class II malocclusion plays an important role in
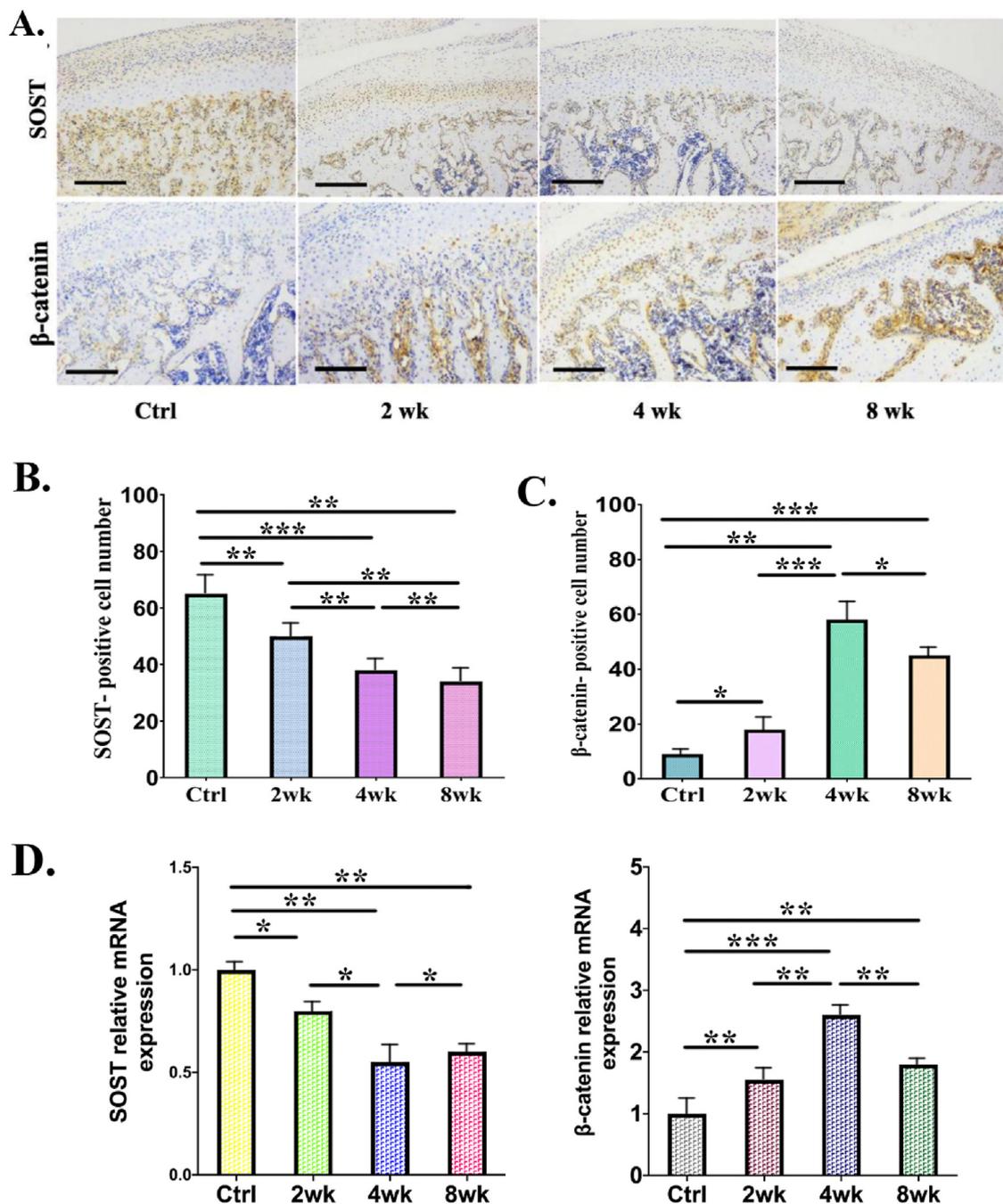
6

Figure 6. A: Decreased expression of sclerostin (SOST), and increased expression of β-catenin at the mandibular condyles in the control and overloading groups. **A-C**: Immunohistochemistry for SOST and β-catenin in sagittal sections of condyles. Scale bar = 50 μm. **D**: The results of RT-PCR analysis and the relative expression of SOST and β-catenin. $*P < 0.05$; $**P < 0.01$; $***P < 0.001$.

stimulating condyle growth [19]. In this experimental study, mandible advancement (MA) appliances were used to mandibular advancement among SD rats over 8 weeks period. This study chose rat model due to it is similar to human in the morphological, anatomical and structural of condyles.

Previous studies [20] indicated that mandible advancement (MA) appliances could transfer functional orthopedic force to the mandibular condyle, and modulate cartilage growth and bone formation. But the main pathologic change in TMJ-OA is overloading stress induced condylar cartilage degeneration [16]. Therefore, the effect of overloading on articular cartilage and subchondral bone caused by TMJ OA raises our concern.

In this study, we made a mandibular advancement appliance to establish OFOF model in rats and TMJ-OA model was successfully induced by OFOF. There are many studies that using different methods to make mandibular forward models, in Rabie's research, the appliances that were fitted to the upper incisors of animals [21], unlike their appliances, ours was fixed to the rat's maxilla by elastic traction, and neck fixation device was used to assist the fixation to avoiding fall off; In the Crossman's study, the collagen induced arthritis (CIA) juvenile rat model was used, and the articular condyle cartilage of the CIA group underwent degenerative changes, this method adopted injection, which was simple and feasible [22]. In contrast, our model adopted physical means to force the mandible of rats to extend forward, simulating the process of

mechanical force overload of joints. Studies have shown that the fibrous layer of normal condyle is continuous and smooth, and chondrocytes are oriented in an orderly manner; whereas chondrocytes in pathological condition are disordered and the number of chondrocytes are significantly reduced even eliminated [23]. Similar pathological changes also occurred in the OFOF rat model in this study.

To further explore how overloaded functional orthopedic force induces pathological changes of condylar cartilage, we investigated the expression level of COL-2 and MMP-3. In the normal conditions, abundant collagen and proteoglycans compose the cartilage matrix [24]. COL-2 accounts for more than 90% of total collagen, which can maintain the organic morphology of cartilage tissue and also become the microenvironment for chondrocyte metabolism [25]. The metabolic activity and health of cartilage can be visualized by COL-2 [26]. In this study, the expression level of COL-2 was significantly reduced in the orthotic force overloaded rat model. MMPs is a proteolytic enzyme widely existing in connective tissue, which plays an important regulatory role in physiological reconstruction and pathological destruction [27]. MMP-3 is an important hydrolase which can activate multifarious MMP precursors, gelatinases and collagenases, with the ability to degrade cartilage and bone extracellular matrix [28]. It's level was consistent with cartilage damage [29, 30]. In this study, overloading effectively increased the expression level of MMP-3 in damaged condylar cartilage. In addition, the expression of COL-2 was negatively correlated with MMP-3, indicating that the degradation of COL-2 was related to MMP-3 closely. However, how overload affects MMP-3 expression remains unclear.

Chondrodegeneration and destruction of subchondral bone can be caused by abnormal death of chondrocytes. The cartilage is tightly attached to the subchondral bone to form a functional unit which called the osteochondral junction, and the osteochondral junction includes the area between the deeper articular cartilage and the underlying subchondral bone and, changing any of these tissues alters the rest of the complex; during joint load bear process, cartilage and subchondral bone play complementary roles [31]. Subchondral bone supports cartilage, which can transfer increased load to the upper cartilage, leading to secondary cartilage damage and degenerative changes [5]. After cartilage injury, the load transferred to the subchondral bone also increases [32]. The performance of cartilage and subchondral bone in TMJOA rats in this study also conforms to this theory. Abnormal remodeling of subchondral bone is one of the earliest pathological features of TMJ osteoarthritis. In the early stage of TMJ osteoarthritis, subchondral bone is mainly characterized by bone loss, followed by slow repair activity that increases subchondral bone mass. Many molecular signaling pathways in endochondral ossification are involved in temporomandibular joint osteoarthritis.

The classic Wnt/β-catenin signaling pathway not only plays an important role in the regulation of bone metabolic balance, but also is the key to regulating the pathogenesis of arthritis. Activation of the Wnt/β-catenin signaling pathway is thought to be responsible for excessive remodeling and the degradation of cartilage matrix in pathology [33]. As described in detail previously [34, 35], overexpression of β-catenin has been shown to induce an OA-like phenotype and significantly affect the expression of chondrocyte marker genes such as MMPs, ADAMTs, aggrecan and type II collagen. Molecular or pharmacological agents that inhibit the Wnt/β-catenin signaling pathway in chondrocytes reduce expression of stromal regulatory enzymes, including MMPs, which may help slow disease progression of OA. Besides, increased Wnt signaling inhibits chondrogenesis [36]. Sclerostin, an inhibitor of the Wnt/β-catenin signaling pathway, is expressed in chondrocytes and regulates chondrogenic differentiation [37]. In this study, mechanical load activates the Wnt/β-catenin signaling pathway through downregulation of sclerostin in temporomandibular joint OA progression induced by overloaded force. Wnt/β-catenin signaling pathway is activated in the progress of mandibular condylar cartilage degeneration and subchondral bone loss induced by OFOF.

Studies have shown that cartilage homeostasis requires a delicate balance of WNT activity because both inhibition [38] and constructive activation [39] of the β-catenin pathway lead to cartilage breakdown. Similarly, excessive WNT activation following loss of WNT inhibitor function leads to increased susceptibility to OA in humans [40], but excessive WNT inhibition due to tumor necrosis factor-dependent DKK1 expression in inflammatory arthritis leads to cartilage and bone destruction. How this balance is achieved within the joint is unclear. Chen's study showed the evidence that the Wnt signaling components were involved in the development of the condylar cartilage. Furthermore, the expression of the Wnt components was predominant at the developmental stages, compared to adult period, indicating the importance of Wnt signaling for chondrogenesis and morphogenesis of condylar cartilage [41]. Martijn H's data show that canonical Wnts, which overexpressed in the synovium during experimental OA, may conduce to OA pathology [42]. Therefore regulation of Wnt and Wnt antagonists have emerged as a potential strategy to influence tissue remodelling and regeneration in degenerative joint diseases such as OA.

5. Conclusion

The results indicated that Wnt/β-catenin signaling pathway may have a certain effect on TMJ OA. In short, Wnt signal transduction has been proven to bone involved in bone formation and bone resorption, and also plays an important role in bone metabolism. Since the Wnt/β-catenin signaling pathway participating in the subchondral bone of the condyle, the development of biological products related to the Wnt/β-catenin signaling pathway inhibitor to reduce the occurrence of TMJ OA is undoubtedly a beneficial treatment attempt. Therefore, these results suggested that Wnt/β-catenin signaling pathway is activated in the progress of mandibular condylar cartilage degeneration and subchondral bone loss induced by overloaded functional orthopedic force (OFOF).

Declarations

Author contribution statement

Zijing He: Performed the experiments; Analyzed and interpreted the data; Wrote the paper.

Meixi Liu: Conceived and designed the experiments; Performed the experiments; Analyzed and interpreted the data.

Qiang Zhang: Conceived and designed the experiments; Analyzed and interpreted the data.

Yihong Tian: Conceived and designed the experiments; Performed the experiments.

Lingzhi Wang; Xiao Yan; Dapeng Ren: Analyzed and interpreted the data.

Xiao Yuan: Conceived and designed the experiments; Analyzed and interpreted the data; Contributed reagents, materials, analysis tools or data.

Data availability statement

Data will be made available on request.

Declaration of interests statement

The authors declare no conflict of interest.

Additional information

No additional information is available for this paper.

References

[1] J. Paulose, P.J. Antony, B. Sureshkumar, S.M. George, M.M. Mathew, J. Sebastian, PowerScope a Class II corrector - a case report, Contemp. Clin. Dent. 7 (2) (2016) 221–225.

[2] H. Pancherz, S. Ruf, P. Kohlhas, Effective condylar growth and chin position changes in Herbst treatment: a cephalometric roentgenographic long-term study, Am. J. Orthod. Dentofacial Orthop. 114 (4) (1998) 437–446.

[3] I. Mizoguchi, I. Takahashi, M. Nakamura, et al., An immunohistochemical study of regional differences in the distribution of type I and type II collagens in rat mandibular condylar cartilage, Arch. Oral Biol. 41 (8-9) (1996) 863–869.

[4] H.U. Luder, C.P. Leblond, K. von der Mark, Cellular stages in cartilage formation as revealed by morphometry, radioautography and type II collagen immunostaining of the mandibular condyle from weanling rats, Am. J. Anat. 182 (3) (1988) 197–214.

[5] M.B. Goldring, S.R. Goldring, Articular cartilage and subchondral bone in the pathogenesis of osteoarthritis, Ann. N. Y. Acad. Sci. 1192 (2010) 230–237.

[6] H. Tabeian, B.F. Betti, C. dos Santos Cirqueira, et al., Il-1β damages fibrocartilage and upregulates mmp-13 expression in fibrochondrocytes in the condyle of the temporomandibular joint, Int. J. Mol. Sci. 20 (9) (2019) 1–15.

[7] T. Fujisawa, T. Kuboki, T. Kasai, et al., A repetitive, steady mouth opening induced an osteoarthritis-like lesion in the rabbit temporomandibular joint, J. Dent. Res. 82 (9) (2003) 731–735.

[8] J. Zhang, K. Jiao, M. Zhang, et al., Occlusal effects on longitudinal bone alterations of the temporomandibular joint, J. Dent. Res. 92 (3) (2013) 253–259.

[9] M.J. Ravosa, R. Kunwar, S.R. Stock, M.S. Stack, Pushing the limit: masticatory stress and adaptive plasticity in mammalian craniomandibular joints, J. Exp. Biol. 210 (4) (2007) 628–641.

[10] E. Tanaka, J. Aoyama, M. Miyauchi, et al., Vascular endothelial growth factor plays an important autocrine/paracrine role in the progression of osteoarthritis, Histochem. Cell Biol. 123 (3) (2005) 275–281.

[11] T. Sobue, W.C. Yeh, A. Chhibber, et al., Murine TMJ loading causes increased proliferation and chondrocyte maturation, J. Dent. Res. 90 (4) (2011) 512–516.

[12] A. Utreja, N. Dyment, S. Yadav, et al., Cell and matrix response of temporomandibular cartilage to mechanical loading, Osteoarthritis Cartilage 24 (2016) 335–344.

[13] J. Yang, Y. Li, Y. Liu, et al., Role of the SDF-1/CXCR4 signaling pathway in cartilage and subchondral bone in temporomandibular joint osteoarthritis induced by overloaded functional orthopedics in rats, J. Orthop. Surg. Res. 15 (1) (2020) 1–11.

[14] S.S. Glasson, M.G. Chambers, W.B. Van Den Berg, C.B. Little, The OARSI histopathology initiative - recommendations for histological assessments of osteoarthritis in the mouse, Osteoarthritis Cartilage 18 (SUPPL. 3) (2010) S17–S23.

[15] M. Thomas, Z. Fronk, A. Gross, et al., Losartan attenuates progression of osteoarthritis in the synovial temporomandibular and knee joints of a chondrodysplasia mouse model through inhibition of TGF-β1 signaling pathway, Osteoarthritis Cartilage 27 (4) (2019) 676–686.

[16] L. Fang, Y. Ye, X. Tan, L. Huang, Y. He, Overloading stress–induced progressive degeneration and self-repair in condylar cartilage, Ann. N. Y. Acad. Sci. 1503 (1) (2021) 72–87.

[17] T. Izawa, H. Mori, T. Shinohara, et al., Rebamipide attenuates mandibular condylar degeneration in a murine model of TMJ-OA by mediating a chondroprotective effect and by downregulating RANKL-mediated osteoclastogenesis, PLoS One 11 (4) (2016) 162032.

[18] G. Zeng, B. Kuang, Xun W. xing, Ren G. tong, Wei K. wen, Response of mandibular condyles of juvenile and adult rats to abnormal occlusion and subsequent exemption, Arch. Oral Biol. 80 (2017) 136–143.

[19] R. Oksayan, O. Sokucu, N. Ucuncu, Effects of bite-jumping appliances on mandibular advancement in growing rats: a radiographic study, Eur. J. Dermatol. 8 (3) (2014) 291–295.

[20] W.F. Franco, M.V.B. Galdino, L.R. Capeletti, et al., Photobiomodulation and mandibular advancement modulates cartilage thickness and matrix deposition in the mandibular condyle, Photobiomod. Photomed. Laser Surg. 38 (1) (2020) 3–10.

[21] A.B.M. Rabie, Z. Zhao, G. Shen, E.U. Hägg, W. Robinson, Osteogenesis in the glenoid fossa in response to mandibular advancement, Am. J. Orthod. Dentofacial Orthop. 119 (4) (2001) 390–400.

[22] J. Crossman, H. Lai, M. Kulka, N. Jomha, P. Flood, T. El-Bialy, Collagen-induced temporomandibular joint arthritis juvenile rat animal model, Tissue Eng. C Methods 27 (2) (2021) 115–123.

[23] C. Liang, T. Yang, G. Wu, J. Li, W. Geng, The optimal regimen for the treatment of temporomandibular joint injury using low-intensity pulsed ultrasound in rats with chronic sleep deprivation, BioMed Res. Int. 2020 (2020) 5468173.

[24] A. Nazempour, B.J. Van Wie, Chondrocytes, mesenchymal stem cells, and their combination in articular cartilage regenerative medicine, Ann. Biomed. Eng. 44 (5) (2016) 1325–1354.

[25] J. Crossman, N. Alzaheri, M.N. Abdallah, et al., Low intensity pulsed ultrasound increases mandibular height and Col-II and VEGF expression in arthritic mice, Arch. Oral Biol. 104 (February) (2019) 112–118.

[26] M. Simental-Mendía, J. Lara-Arias, E. Álvarez-Lozano, et al., Cotransfected human chondrocytes: over-expression of IGF-I and SOX9 enhances the synthesis of cartilage matrix components collagen-II and glycosaminoglycans, Braz. J. Med. Biol. Res. 48 (12) (2015) 1063–1070.

[27] T. Fukui, E. Tenborg, J.H. Yik, D.R. Haudenschild, In-vitro and in-vivo imaging of MMP activity in cartilage and joint injury, Biochem. Biophys. Res. Commun. 460 (3) (2015) 741–746.

[28] J. Yu, E. Mursu, M. Typpö, et al., MMP-3 and MMP-8 in rat mandibular condylar cartilage associated with dietary loading, estrogen level, and aging, Arch. Oral Biol. 97 (July 2018) (2019) 238–244.

[29] S. Sun, A.C. Bay-Jensen, M.A. Karsdal, et al., The active form of MMP-3 is a marker of synovial inflammation and cartilage turnover in inflammatory joint diseases, BMC Muscoskel. Disord. 15 (1) (2014) 1–8.

[30] D.J. Leong, X.I. Gu, Y. Li, et al., Matrix metalloproteinase-3 in articular cartilage is upregulated by joint immobilization and suppressed by passive joint motion, Matrix Biol. 29 (5) (2010) 420–426.

[31] S. Suri, D.A. Walsh, Osteochondral alterations in osteoarthritis, Bone 51 (2) (2012) 204–211.

[32] T. Neogi, M. Nevitt, J. Niu, et al., Subchondral bone attrition may be a reflection of compartment- specific mechanical load: the MOST Study, Ann. Rheum. Dis. 69 (5) (2010) 841–844.

[33] T. Yuasa, T. Otani, T. Koike, M. Iwamoto, M. Enomoto-Iwamoto, Wnt/β-catenin signaling stimulates matrix catabolic genes and activity in articular chondrocytes: its possible role in joint degeneration, Lab. Invest. 88 (3) (2008) 264–274.

[34] B.Y. Chan, E.S. Fuller, A.K. Russell, et al., Increased chondrocyte sclerostin may protect against cartilage degradation in osteoarthritis, Osteoarthritis Cartilage 19 (7) (2011) 874–885.

[35] J. Wu, L. Ma, L. Wu, Q. Jin, Wnt-β-catenin signaling pathway inhibition by sclerostin may protect against degradation in healthy but not osteoarthritic cartilage, Mol. Med. Rep. 15 (5) (2017) 2423–2432.

[36] H. Yu, Y. Liu, X. Yang, et al., Strontium ranelate promotes chondrogenesis through inhibition of the Wnt/β-catenin pathway, Stem Cell Res. Ther. 12 (1) (2021) 1–14.

[37] L. Ma, Y. Liu, X. Zhao, P. Li, Q. Jin, Rapamycin attenuates articular cartilage degeneration by inhibiting β-catenin in a murine model of osteoarthritis, Connect. Tissue Res. 60 (5) (2019) 452–462.

[38] M. Zhu, M. Chen, M. Zuscik, et al., Inhibition of beta-catenin signaling in articular chondrocytes results in articular cartilage destruction, Arthritis Rheum. 58 (2008) 2053–2064.

[39] M. Zhu, D. Tang, Q. Wu, et al., Activation of beta-catenin signaling in articular chondrocytes leads to osteoarthritis-like phenotype in adult beta-catenin conditional activation mice, J. Bone Miner. Res. 24 (2009) 12–21.

[40] J. Loughlin, B. Dowling, K. Chapman, et al., Functional variants within the secreted frizzled-related protein 3 gene are associated with hip osteoarthritis in females, Proc. Natl. Acad. Sci. U.S.A. 101 (2004) 9757–9762.

[41] Kan Chen, Huixin Quan, Gang Chen, et al., Spatio-temporal expression patterns of Wnt signaling pathway during the development of temporomandibular condylar cartilage, Gene Expr. Patterns 25–26 (2017) 149–158.

[42] H. Martijn, van den Bosch, B. Arjen, Annet W. Blom, et al., Induction of canonical Wnt signaling by synovial overexpression of selected Wnts leads to protease activity and early osteoarthritis-like cartilage damage, Am. J. Pathol. 185 (7) (2015).